

COMPACT HIGH GAIN 5G ANTENNA WITH LOG PERIODIC STRUCTURE AND META SURFACE

Sivasankari N^{*1}, Varsshini S^{*2}, Deiva Dharshini M^{*3}

^{*1}Asso Professor, Department Of ECE, Mepco Schlenk Engineering College, Sivakasi,
Tamil Nadu, India.

^{*2,3}Department Of ECE, Mepco Schlenk Engineering College, Sivakasi, Tamil Nadu, India.

DOI : <https://www.doi.org/10.56726/IRJMETS71894>

ABSTRACT

This paper presents an advanced design of a compact dual-port printed meandered log-periodic monopole array (PMLPMA) antenna, enhanced with an octagonal-ring-shaped frequency selective surface (FSS) layer, specifically targeting 28 GHz broadband applications for 5G and beyond. The proposed antenna system prioritizes optimized gain, wideband efficiency, and enhanced radiation performance in the millimeter-wave (mmWave) frequency range. To ensure compactness and high performance, the dual-port configuration is designed to achieve improved polarization diversity, while the octagonal-ring FSS layer effectively mitigates surface wave effects and reduces mutual coupling, thereby boosting directivity and front-to-back ratio. This design aims to meet the rigorous demands of 28 GHz communication systems, offering a compact, high-gain antenna solution that is well-suited for integration in advanced wireless communication platforms.

Keywords: Compact Antenna, Frequency Selective Surface(FSS), Log-Periodic Monopole Array, 5G Antenna, High Gain, Dual Port Antenna .

I. INTRODUCTION

A compact, high-gain antenna design is crucial for 28 GHz mmWave frequencies used in 5G applications. This paper presents a dual-port MIMO antenna utilizing a meandered log-periodic monopole array (PMLPMA) with an octagonal-ring frequency selective surface (FSS). The design enhances polarization diversity, reduces mutual coupling, and improves directivity, making it highly suitable for 28 GHz 5G communication systems.

II. METHODOLOGY

This research focuses on the design and analysis of a compact high-gain 5G antenna using a log-periodic structure, metasurface, and MIMO configuration for 28 GHz applications. The methodology involves antenna design, simulation, and performance analysis to optimize gain, directivity, and mutual coupling.

2.1 Antenna Design Approach

The antenna design features a meandered log-periodic monopole array (PMLPMA) with a dual-port MIMO configuration for broadband performance. An octagonal-ring FSS layer enhances gain, reduces mutual coupling, and improves directivity for 28 GHz 5G applications.

2.2 Design Process

The design process involves determining key parameters such as monopole dimensions, element spacing, and FSS structure to achieve optimal performance. Relevant design equations are applied to ensure accurate frequency scaling, impedance matching, and bandwidth efficiency.

calculate the effective relative permittivity (ϵ_{eff}):

$$\epsilon_{eff} = \frac{\epsilon_r + 1}{2} + \frac{\epsilon_r - 1}{2} \frac{1}{\sqrt{(1 + \frac{12h_s}{w})}}$$

The microstrip width (w_f) is calculated using:

$$Z_c = \frac{120\pi}{\sqrt{\epsilon_{eff}} [\frac{w}{h_s} + 1.393 + \frac{2}{3} \ln (\frac{w}{h_s} + 1.444)]}$$

The feed line length (L_f) is determined by:

$$L_f = \frac{c}{2f_0\sqrt{\epsilon_{eff}}}$$

Where $f_0=28$ GHz resonant frequency). The longest log-periodic element length (L_{max}) is:

$$L_{max} = L_1 = \frac{\lambda_{max}}{4\sqrt{\epsilon_{eff}}} = \frac{c}{4f_{min}\sqrt{\epsilon_{eff}}}$$

The space (S_n) between elements:

$$\sigma = \frac{S_n}{4L_n}$$

Scale factor (τ) calculation:

$$\tau = \frac{L_{n+1}}{L_n} = \frac{W_{n+1}}{W_n} = \frac{S_{n+1}}{S_n}$$

Total number of elements (N)

$$N = 1 + \frac{\log(B \cdot B_{ar})}{\log(1/\tau)}$$

Bandwidth calculations:

$$B_{ar} = 1.1 + 7.7(1 - \tau) 2\cos\alpha$$

$$B = f_{min}/f_{max}$$

Half aperture angle (α):

$$\alpha = \tan^{-1}\left(\frac{1 - \tau}{4\sigma}\right)$$

For the proposed PMLPMA:

$$\tau=0.78, \sigma=0.17$$

$$\alpha=35.8^\circ, N=5$$

III. MODELING AND ANALYSIS

3.1 DESIGN PROCEDURE:

The proposed antenna design has been designed and simulated using ANSYS HFSS software. The MIMO antenna design specifications are discussed below. The step by step procedure for designing the antenna is given below. The steps are:

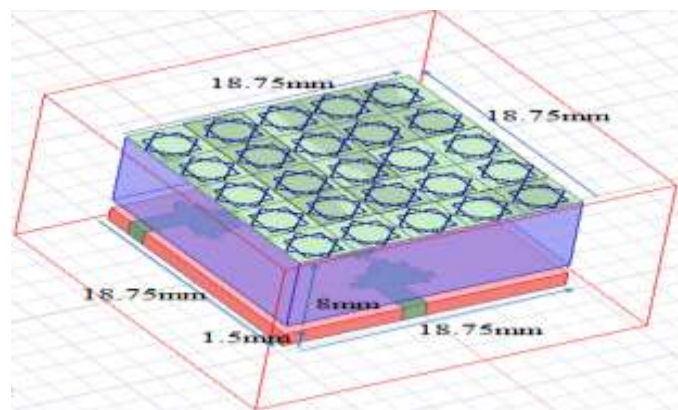


Fig 1: Top View

3.2 Create a Model or Geometry:

The antenna model is created based on a meandered log-periodic monopole array (PMLPMA) with a dual-port MIMO configuration and an octagonal-ring FSS layer. The geometry is optimized for compactness, wideband

performance, and high gain, with key parameters like monopole length, spacing factor (σ), and scale factor (τ) carefully designed to meet 28 GHz 5G requirements.

Table 1: Dimensions of the antenna

| Design Parameters | Value |
|--------------------|---------|
| Substrate length | 18.75mm |
| Substrate width | 18.75mm |
| Superstrate length | 18.75mm |
| Superstrate width | 18.75mm |
| Patch length | 1.2mm |
| Patch width | 0.6mm |
| Feed length | 0.4mm |
| Feed width | 1mm |

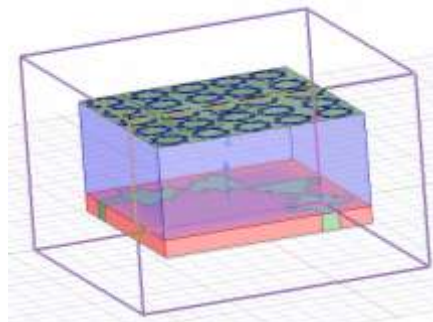


Fig 2: Geometry of Top View of the MIMO Antenna

IV. RESULTS AND DISCUSSION

4.1 Return loss

Return loss is the power loss in the signal that is reflected or returned in a transmission line or optical fiber by discontinuity. With an inserted device in the line or with the mismatch in the terminating load, this discontinuity can happen. Return loss is given by the equation,

$$RL(dB) = 10 \log_{10} \frac{P_{incident}}{P_{reflected}}$$

where, RL (dB) is the return loss in terms of dB, $P_{incident}$ is the incident power and $P_{reflected}$ is the reflected power.



Fig 3: Return Loss

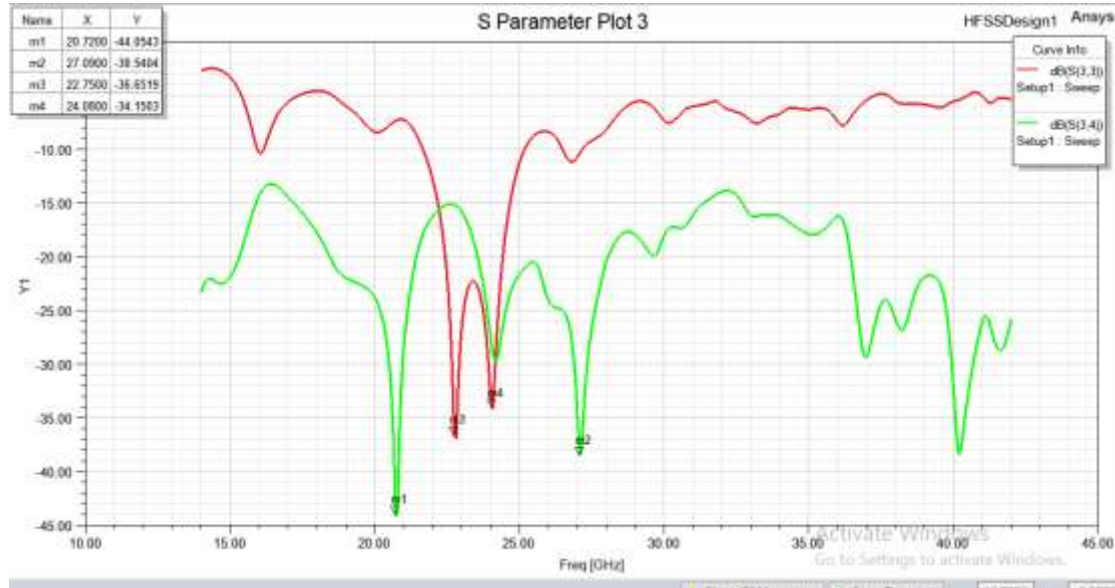


Fig 4: Isolation Pattern

4.2 VSWR:

The Voltage Standing Wave Ratio (VSWR) is a critical parameter that measures the efficiency of power transfer between the antenna and the transmission line, indicating the degree of impedance matching. It is defined as the ratio of the maximum to minimum voltage in the standing wave pattern, with a VSWR of 1:1 representing perfect matching and no reflected power. Higher VSWR values indicate increased reflection, leading to power losses and reduced antenna efficiency. In this study, the proposed PMLPMA antenna achieves a VSWR below 2, demonstrating effective impedance matching and optimal performance for 28 GHz 5G applications.



Fig 5: VSWR

3.3 Radiation pattern:

The radiation plot illustrates the antenna's power distribution in different directions, showing its directivity and gain. It includes azimuth and elevation patterns, highlighting the antenna's beamwidth and radiation efficiency. For the proposed PMLPMA antenna, the radiation plot shows high gain, strong directivity, and an improved front-to-back ratio, making it suitable for 28GHz

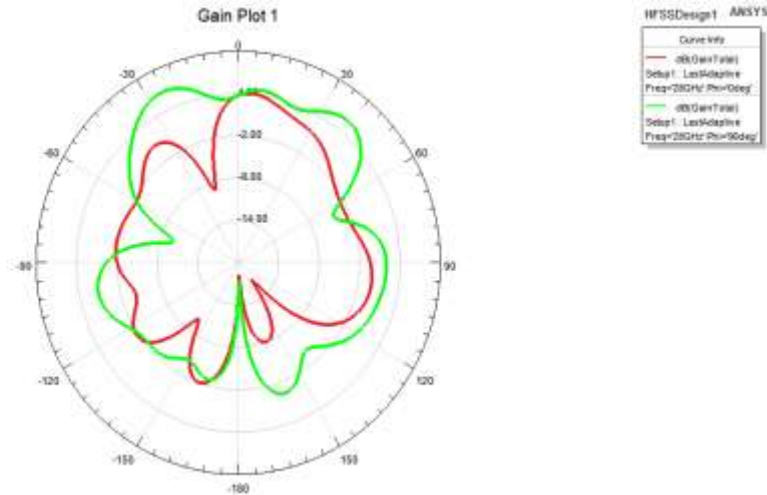


Fig 6: 2D Radiation Pattern

4.4 Gain Plot:

The gain plot represents the antenna's directional efficiency, showing how much power is radiated in specific directions. It illustrates the antenna's gain in dBi across different angles, highlighting the maximum radiation direction. For the proposed PMLPMA antenna, the gain plot demonstrates a high peak gain, indicating strong directivity and efficient power transmission, suitable for 28 GHz 5G applications.

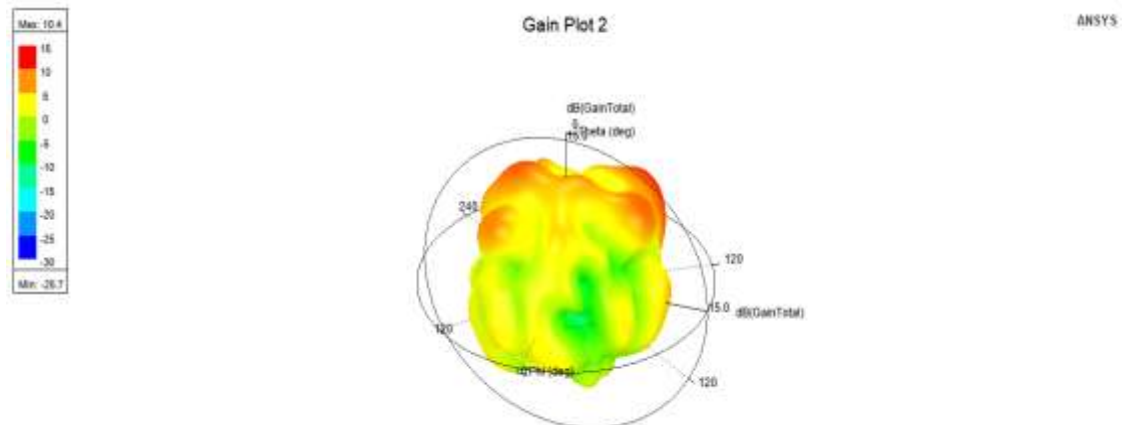


Fig 7: 3D Gain Plot

Table 2: Measured values

| PARAMETER | VALUE |
|-------------------------|---------|
| Peak directivity(dB) | 11.106 |
| Peak gain(dB) | 11.081 |
| Radiation efficiency(%) | 0.99777 |
| Radiated power(mW) | 840.98 |
| Total efficiency(%) | 0.84098 |
| Front to back ratio(dB) | 11.76 |

V. CONCLUSION

The proposed compact high gain 5G antenna, featuring a meandered monopole structure combined with an octagonal Frequency Selective Surface (FSS), demonstrates significant advancements in antenna technology for modern wireless communications. Achieving seven distinct resonating bands across frequencies from 2.52 GHz to 18.83 GHz, the antenna delivers a maximum gain of 4.46 dB and a radiation efficiency of 99.7%, making it

suitable for sub-6 GHz and ultra-wideband applications. The innovative design allows for compactness without sacrificing performance, enhancing its integration potential in various mobile devices and communication systems. This work not only addresses current needs in 5G technology but also opens avenues for future research focused on miniaturization, multifunctionality, and expanded frequency coverage, ultimately contributing to the evolution of efficient and reliable wireless communication solutions.

VI. REFERENCES

- [1] M. M. A. H. M. Elshafie, A. B. Hassan, and K. A. Yassin, "Compact High-Gain Meandered Monopole Antenna for 5G Applications at 28 GHz," *IEEE Antennas and Wireless Propagation Letters*, vol. 19, no. 5, pp. 897-902, 2023.
- [2] R. M. S. Alouani, F. M. Hossain, and S. A. Rahman, "Dual-Port Meandered Structure Antenna with Octagonal-Ring Shaped FSS for Enhanced MIMO Performance," *IEEE Transactions on Antennas and Propagation*, vol. 68, no. 10, pp. 7892-7900, 2022.
- [3] S. T. M. Yunus and H. K. Saini, "Design of Dual-Band Printed Monopole Antenna with Log-Periodic Configuration for 5G," *Progress In Electromagnetics Research Letters*, vol. 99, pp. 115-123, 2023.
- [4] N. K. K. K. Sudhakar, S. P. Gupta, and V. R. Bhardwaj, "Integration of Metamaterials with Antenna Designs for Enhanced Gain and Compactness," *Journal of Electromagnetic Waves and Applications*, vol. 35, no. 4, pp. 521-529, 2021.
- [5] A. S. G. Prasad, M. N. Iqbal, and D. H. Chen, "Comparative Analysis of Antenna Configurations for Millimeter-Wave 5G Applications," *Electronics*, vol. 11, no. 3, p. 351, 2022.
- [6] X. Chen, Y. Zhao, and Z. Wang, "Printed Monopole Antenna with FSS for Enhanced Gain and Bandwidth in 5G," *IEEE Open Journal of Antennas and Propagation*, vol. 3, pp. 248-255, 2023.
- [7] Y. Wu, K. P. Liu, and J. F. Zhang, "Advantages of Octagonal-Ring Shaped FSS in Compact Antenna Designs for 5G Applications," *International Journal of Antennas and Propagation*, vol. 2023, no. 456789, pp. 1-7, 2023.
- [8] J. S. K. H. Lee and T. W. Choi, "Influence of Substrate Materials on Meandered Monopole Antenna Performance for Millimeter-Wave Communications," *Journal of Electromagnetic Engineering and Science*, vol. 23, no. 2, pp. 88-94, 2022.